Journal of Applied Polymer Science

Viscoelastic Behavior of Hybrid Building Materials

George Christopher Papanicolaou,[1] Georgios P. Lagas,[1] Stefanos Polymeros Zaoutsos[2]

[1]Composite Materials Group, Department of Mechanical and Aeronautics Engineering, University of Patras, GR-26500 Patras, Greece

[2]Laboratory of Advanced Materials and Constructions, Department of Mechanical Engineering, Technological Educational Institute of Thessaly, GR-41110 Larissa, Greece

Correspondence to: G. C. Papanicolaou (E-mail: gpapan@mech.upatras.gr)

ABSTRACT: The objective of this experimental work is the investigation of the viscoelastic behavior of a hybrid matrix, fiber-reinforced building material. Hybrid matrix consisted of epoxy resin mixed with fine marble sand, whereas short steel fibers were used as reinforcement. The experimental procedure involved, first, the manufacturing of specimens using different hybrid matrix types and different reinforcement by weight ratios. Subsequently, bending relaxation experiments at room temperature were executed, under three-point bending test experimental configuration, at different strain levels and the variation of stress of the hybrid matrix material with time was monitored. The data obtained were used to (i) investigate the effect of reinforcement mass fraction contained in the composite on the viscoelastic behavior and (ii) to apply existed and newly developed viscoelastic models for the description of the observed viscoelastic behavior. More precisely, the four-parameter (Burgers) viscoelastic model and the modified Residual Property Model were calibrated and used to simulate the relaxation behavior of the materials manufactured and tested. Experimental results exhibited a clear influence of both reinforcement ratio and initial displacement on the viscoelastic behavior of the materials manufactured and tested, whereas the models proposed and used can adequately reproduce the variation of relaxation stress with time. © 2014 Wiley Periodicals, Inc. J. Appl. Polym. Sci. **2015**, *132*, 41429.

KEYWORDS: composites; fibers; theory and modeling; viscosity and viscoelasticity

Received 19 June 2014; accepted 20 August 2014

DOI: 10.1002/app.41429

INTRODUCTION

Although primarily reluctant, due mainly to high cost, building industry has nowadays implemented the use of polymers and polymer–matrix composites in many of its aspects. Either in constructing new or repairing and strengthening existing technical works, the use of polymers and polymer matrix composites is now a common practice.[1]

Carbon or glass fabrics and plates attached to an existing concrete member by means of a polymer matrix are examples of polymer matrix composites used for restoration and enhancement of the bearing capability of existing structures.[2–5] In other cases, polymer composites can be used to substitute traditional building materials. For example, steel rebars are substituted in some applications, by continuous glass of carbon fibers inside a polymer matrix, formed in the shape of a rebar in various diameter sizes.[6] Polymers are also used in the building industry. For example, low-viscosity epoxy resin is used to repair cracks on a concrete structure because of severe earthquake loading.[7]

Concrete modification or substitution using polymers is not a new idea. Because of the fact that conventional, cementitious, concrete is subjected to carbonation procedure, which is responsible for severe degradation of the mechanical properties of both concrete and steel rebars,[8–10] a number of solutions was proposed and investigated. Polymer-impregnated concrete,[11] polymer modified concrete (PMC),[12,13] and polymer concrete (PC)[14,15] are the main propositions that were made. Currently, only PMC and PC are still in a status of wide usage.[16]

PC's main difference from regular, cement-based, concrete is that cement is substituted by a polymer matrix. Aggregates with different granulometric characteristics depending on the material application, are used as reinforcement. The resulting product is a low porosity material, which exhibits high strength and stiffness-to-weight ratio, high damping properties, low thermal conductivity, and easy formability through casting.

In previous works,[17] hybrid matrix PC materials reinforced with various types of reinforcements were manufactured. The mechanical behavior of the materials was experimentally investigated by means of three-point bending test. Short steel fibers were found to have a higher, than any other reinforcements used, enhancing effect on both stiffness and flexural strength of

Table I. Compositions of the Manufactured and Tested Hybrid Matrix, Composite Materials

Hybrid matrix	Composition	Epoxy resin (wt %)	Marble sand (wt %)	Steel fibers (wt %)
60% (wt) Marble Sand 40% (wt) Epoxy Resin	M60R40_00	40.00	60.00	0.00
	M60R40_10	36.00	54.00	10.00
	M60R40_20	32.00	48.00	20.00
70% (wt) Marble Sand 30% (wt) Epoxy Resin	M70R30_00	30.00	70.00	0.00
	M70R30_10	27.00	63.00	10.00
	M70R30_20	24.00	56.00	20.00

the material when reinforcement content reached a value of 20 wt %.

Although for conventional, cementitious, concrete viscoelastic behavior is not of critical importance, this does not apply to PC. Polymer matrix response under creep and relaxation conditions is of great significance and should be taken into account.

In the current work, specimens of a hybrid matrix, steel fiber-reinforced material were subjected to stress relaxation test under three-point bending configuration. The experimental results were used to investigate the effect of reinforcement mass fraction in the viscoelastic behavior of the material. Moreover, four-parameter (Burgers) viscoelastic model and modified Residual Property Model (RPM) are used to simulate the relaxation behavior of the material and to predict the stress variation over time.

EXPERIMENTAL

The composite materials that were manufactured and tested in this work consisted of a hybrid matrix reinforced with short steel fibers. Hybrid matrix consisted of epoxy resin and fine marble sand. By mixing these two materials in two by weight ratios, namely 60% marble sand–40% epoxy resin and 70% marble sand–30% epoxy resin. Thus, two types of hybrid matrices were manufactured.

The epoxy resin used is a bisphenol-A epoxy resin which is known under the commercial name RenLam CY219. Polymerization was achieved by the use of proper hardener, commercially known as Ren HY5160, which was added at ratio of 50 wt %, recommended by the producer. The density of the epoxy resin after curing procedure is about 1100.00 kgr/m^3, whereas the modulus of elasticity under three-point bending test was found to be about 3.00 GPa.

Marble sand used basically consists of $CaCO_3$, a by-product of marble process. The marble sand consisted of particles with maximum diameter of 1000 μm, whereas 60% of the particles were in a range of diameters from 250 to 750 μm. The mean value of marble density was approximately 2700.00 kgr/m^3, whereas compressive strength is as high as 140 MPa.

Next, short steel fibers were added as reinforcement to the hybrid matrices. Fibers were 6 mm long with their radius r_f equal to 180 μm manufactured by FIBERTECH under the commercial name ME340. They exhibit a flexural strength of 850 MPa, whereas their modulus of elasticity is about 200 GPa. The density of the steel fibers used is 7800.00 kgr/m^3.

As shown in Table I, different by weight percentages in steel fibers were applied (10 and 20 wt %).

The choice of the compositions presented in Table I was based on the experimental results derived in a previous work[17] where it was found to have an enhanced mechanical behavior compared with the different hybrid matrix compositions and different reinforcement types and contents.

The specimens were manufactured under a standardized procedure which included:

Removal of Humidity from Marble Sand
At this step, marble sand was placed into an oven set to a temperature of 50°C for 24 h. The purpose of this step was all excessive humidity to be expelled from the marble sand, resulting to improved adhesion between epoxy resin and marble sand particles.

Mixing
Mixing procedure, executed by means of an electromechanical mixer set to low rotation speed (500 rpm) because higher speed would cause large quantity of air to be trapped in the mixture, started by the homogenization of the solid ingredients (marble sand and steel fibers). This step was considered to be necessary in achieving a uniform distribution of the reinforcement in the composite. If this step was skipped, considering the low viscosity of the resin, there would be spots of reinforcement agglomerates in the final composite material. When homogenization was accomplished, the liquid part (resin) along with the proper amount of amine (hardener) was added and mixed together with the solid ingredients. Total mixing time was set to 5 min.

Air Removal
Because mechanical mixing results in air insertion, which should be removed, the mixture was placed in a vacuum chamber for a time period of 5 min.

Casting
The mixture was casted in open moulds. The nominal dimensions of the moulds were 100.00 mm in length, 12.90 mm in width, and 3.00 mm in thickness.

Curing
Curing was achieved by 24 h heating in an oven at a constant temperature of 50°C. Next, specimens were placed to an

Table II. Relaxation Stresses (MPa) for the Compositions Manufactured and Tested Under All Initial Displacements Considered

Hybrid matrix	Reinforcement by weight content (%)	Initial displacement (mm)	Time (min)					
			0	15	30	45	60	90
M60R40	0.00	2.00	28.01	24.46	23.07	23.24	23.41	21.76
M60R40	0.00	2.50	39.19	35.43	34.54	33.35	33.00	32.53
M60R40	0.00	3.00	43.56	36.93	34.73	33.29	31.34	28.80
M60R40	10.00	2.00	34.51	27.84	26.45	24.35	24.12	22.19
M60R40	10.00	2.50	48.34	38.58	35.22	33.73	32.23	30.66
M60R40	10.00	3.00	53.93	40.85	37.87	35.46	33.60	31.54
M60R40	20.00	2.00	45.80	38.46	35.96	33.06	32.66	30.97
M60R40	20.00	2.50	51.15	41.92	39.31	37.77	37.06	35.65
M60R40	20.00	3.00	61.16	45.49	41.13	39.45	37.31	36.54
M70R30	0.00	2.00	35.62	30.28	29.37	27.24	26.08	23.56
M70R30	0.00	2.50	45.18	37.79	35.88	34.97	33.32	32.41
M70R30	0.00	3.00	48.10	40.01	37.17	36.28	36.00	34.83
M70R30	10.00	2.00	37.52	32.19	31.29	30.56	29.49	28.52
M70R30	10.00	2.50	48.54	39.57	38.20	35.62	34.97	32.30
M70R30	10.00	3.00	52.07	39.53	37.41	36.72	35.02	34.22
M70R30	20.00	2.00	61.71	47.49	44.08	42.10	39.89	38.18
M70R30	20.00	2.50	69.45	50.05	46.29	42.81	42.46	40.34
M70R30	20.00	3.00	72.06	48.79	44.17	41.53	40.32	37.61

INSTRON 3382 testing machine. The machine was set to three-point bending test configuration. An initial displacement under constant strain rate, equal to 0.5 mm/min, was imposed to the specimen. The force was monitored in 1 min time interval and at the end of the monitoring period a time series of force values was available. Finally, stress values were calculated from the force values resulting to a time series of the relaxation stress. Three different initial displacements were imposed to every composition that was manufactured, namely 2.00, 2.50, and 3.00 mm.

RESULTS AND DISCUSSION

The stress–relaxation experiment is a transient experiment, in which the material is deformed, and the force required to maintain the deformation at a constant value is measured. Thus, the stress required to hold the material at constant deformation dies away with time and is said to relax.

Experimental results for all cases of materials manufactured and tested are shown in Table II, and in Figures 1 and 2, two characteristic cases are graphically shown. Figure 1 depicts flexural stress relaxation variation as a function of time for the M70R30

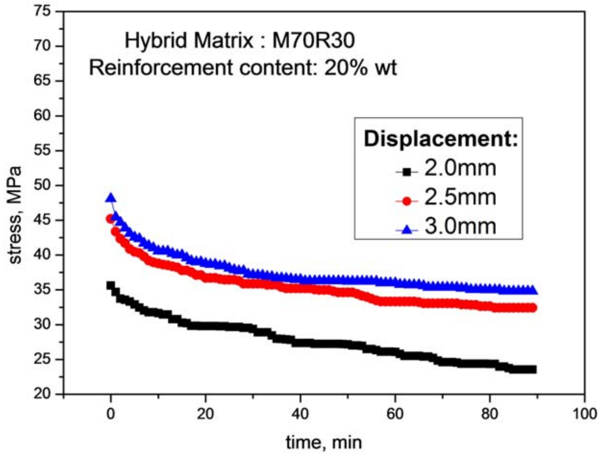

Figure 1. Flexural stress relaxation curves at different displacements for the case of M70R30 hybrid matrix composite reinforced with 20 wt %, steel fibers reinforcement. [Color figure can be viewed in the online issue, which is available at wileyonlinelibrary.com.]

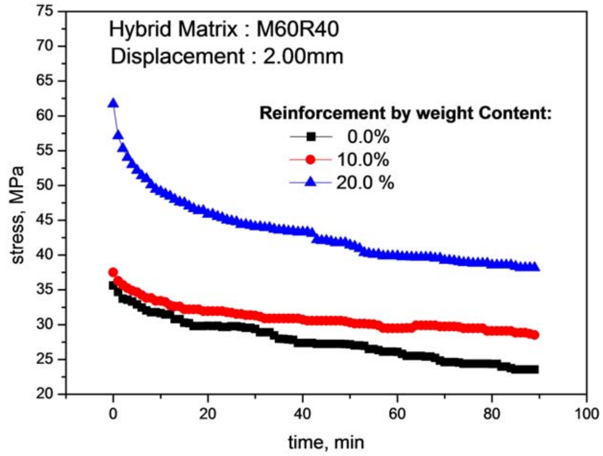

Figure 2. Flexural stress relaxation curves at different, by weight, reinforcement contents for the case of M60R40 hybrid matrix composite at 2.00 mm displacement. [Color figure can be viewed in the online issue, which is available at wileyonlinelibrary.com.]

Table III. Normalized Relaxation Stresses for the Compositions Manufactured and Tested Under All Initial Displacements Considered

Hybrid matrix	Reinforcement by weight content (%)	Initial displacement (mm)	Time (min)					
			0	15	30	45	60	90
M60R40	0.00	2.00	1.00	0.89	0.80	0.79	0.78	0.78
M60R40	10.00	2.00	1.00	0.82	0.72	0.68	0.66	0.64
M60R40	20.00	2.00	1.00	0.84	0.74	0.71	0.69	0.67
M60R40	0.00	2.50	1.00	0.91	0.85	0.84	0.83	0.83
M60R40	10.00	2.50	1.00	0.79	0.70	0.67	0.64	0.63
M60R40	20.00	2.50	1.00	0.82	0.74	0.72	0.70	0.69
M60R40	0.00	3.00	1.00	0.85	0.75	0.72	0.69	0.67
M60R40	10.00	3.00	1.00	0.76	0.66	0.62	0.60	0.58
M60R40	20.00	3.00	1.00	0.74	0.64	0.61	0.59	0.57
M70R30	0.00	2.00	1.00	0.89	0.78	0.74	0.71	0.68
M70R30	10.00	2.00	1.00	0.90	0.84	0.82	0.80	0.79
M70R30	20.00	2.00	1.00	0.77	0.68	0.65	0.63	0.61
M70R30	0.00	2.50	1.00	0.84	0.77	0.74	0.72	0.71
M70R30	10.00	2.50	1.00	0.83	0.74	0.71	0.69	0.67
M70R30	20.00	2.50	1.00	0.73	0.63	0.60	0.59	0.58
M70R30	0.00	3.00	1.00	0.82	0.75	0.74	0.73	0.73
M70R30	10.00	3.00	1.00	0.76	0.70	0.68	0.67	0.66
M70R30	20.00	3.00	1.00	0.68	0.58	0.55	0.54	0.53

hybrid matrix reinforced with 20 wt %, steel fibers at different displacements, whereas in Figure 2, flexural stress relaxation for the M60R40 hybrid matrix reinforced with different reinforcement weight fractions at initial displacement 2.00 mm is shown.

Based on these results, the following conclusions can be deduced:

- An increase in reinforcement by weight ratio causes stress relaxation curves to become parallel and close to each other. In other words, increase in stiffness of the material causes stress to decrease over time with the same rate.

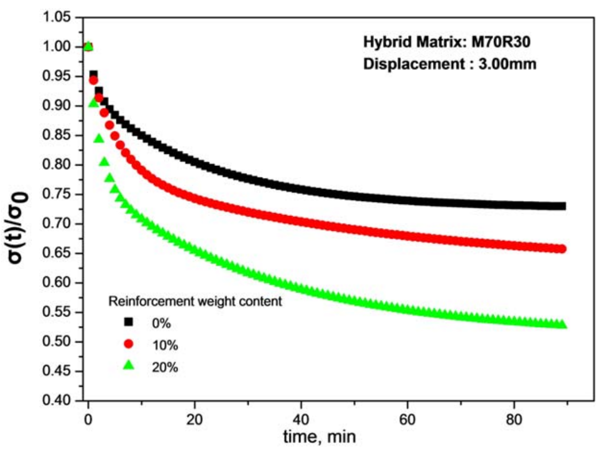

Figure 3. Normalized flexural stress relaxation curves for the M70R70 hybrid matrix at different reinforcement weight concentrations at 3.00 mm displacement. [Color figure can be viewed in the online issue, which is available at wileyonlinelibrary.com.]

- According to the results, in all cases, specimens containing 20% wt reinforcement exhibit higher stress value at the end of the relaxation test period than unreinforced specimens or those containing 10% wt reinforcement. The difference in stress due to higher reinforcement load is more evident at low initial displacements and reduces as displacement increases.

Next, Table III shows the variation of the normalized relaxation stress $(\sigma(t)/\sigma_0)$ over time for the composites based on the M60R40 and M70R30 hybrid matrix, respectively. Figure 3 depicts a characteristic case of normalized relaxation stress variation over time for the M70R30 hybrid matrix at 3.00 mm initial displacement for various by weight reinforcement loading.

It becomes clear for the results that relaxation stress, as a fraction of the initial stress, measured at the end of the relaxation time period, depends on by weight reinforcement content as well as on initial displacement. Increasing the applied displacement or the reinforcement content in the composite leads to a higher stress decrease rate.

As a result, normalized relaxation stress value at the end of the experimental time period is lower as initial displacement imposed and/or by weight reinforcement content is increased.

The main microstructural parameters affecting the mechanical as well as the viscoelastic behavior of the composites manufactured and tested are:

a. The voids created during the mixing procedure.
b. The degree of adhesion between polymer matrix–marble granules and polymer–steel fibers. The higher the adhesion

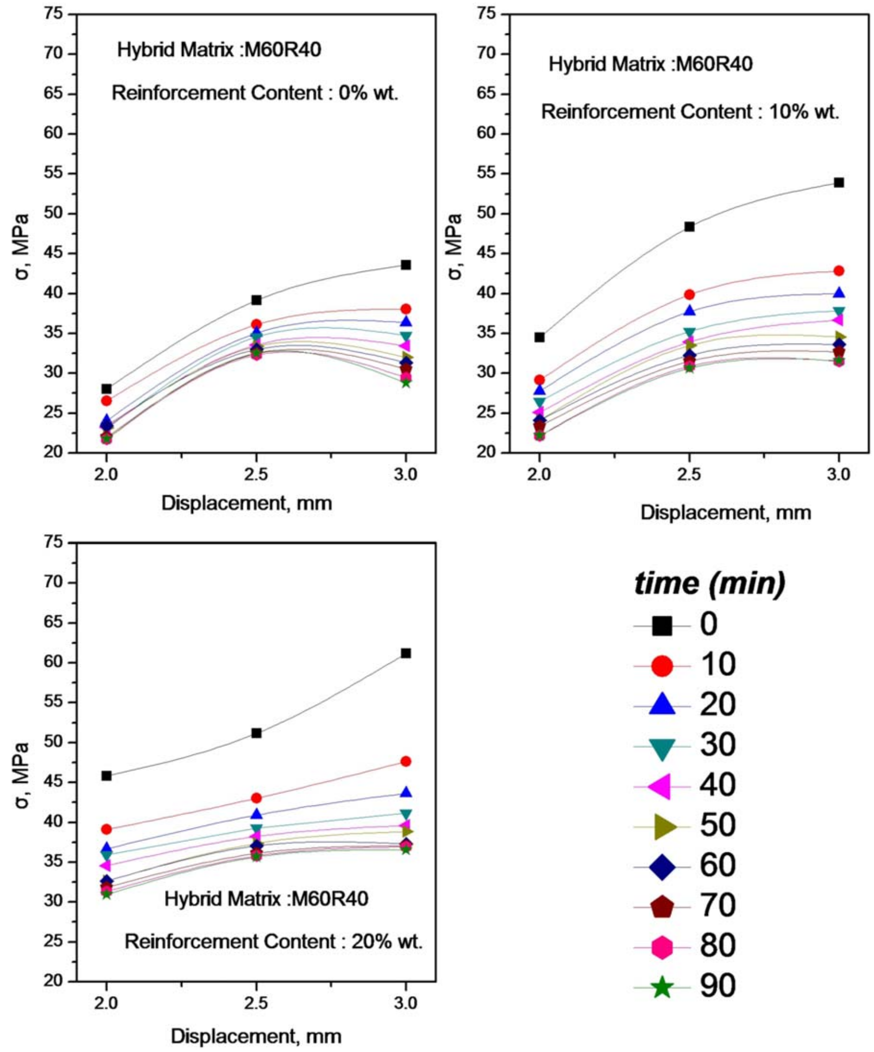

Figure 4. Isochronous curves obtained for the M60R40 hybrid matrix specimens reinforced with short steel fibers at different by weight concentrations. [Color figure can be viewed in the online issue, which is available at wileyonlinelibrary.com.]

bond is, the higher the stress developed in the composite due to initial displacement imposed.

c. The degree of dispersion which in turn depends on the homogenization procedure followed in the stage of mixing.
d. The filler concentration.
e. The fiber agglomeration which is interrelated with the filler concentration, the mixing procedure and the adhesion bond.

From the above-mentioned parameters, it is clear that both the static and the viscoelastic behavior of a hybrid composite is complex, depended on a series of parameters, each one of them being depended on the extend and existence of all the rest.

The importance of the present study is to explore the possibility of using the manufactured and tested hybrid composite in civil engineering structural applications and especially in structural members being under constant displacement working conditions.

In Figures 4 and 5, isochronous curves are shown obtained from the stress relaxation–time curves. Figure 4 shows the isochronous curves corresponding to the materials that were manufactured by adding reinforcement to the M60R40 hybrid matrix, whereas Figure 5 shows the isochronous curves corresponding to composites based on the M70R30 hybrid matrix.

In all cases, a strong nonlinear variation is evident, a fact that implies the intense nonlinear viscoelastic behavior of the materials manufactured and tested.

Despite the fact of nonlinearity, and knowing that models composed of springs and dashpots are solely applicable to materials that exhibit linear viscoelastic behavior, in the sequence, we will apply the four parameters (Burgers) model to our experimental results. In addition, the same experimental results will be modeled by the RPM, which we have developed, for reasons of comparison.

From the above two models, Burgers model is a descriptive model, whereas the RPM is a predictive one. The application of both models to our experimental data will promote the deeper understanding of the materials manufactured and tested in the present investigation.

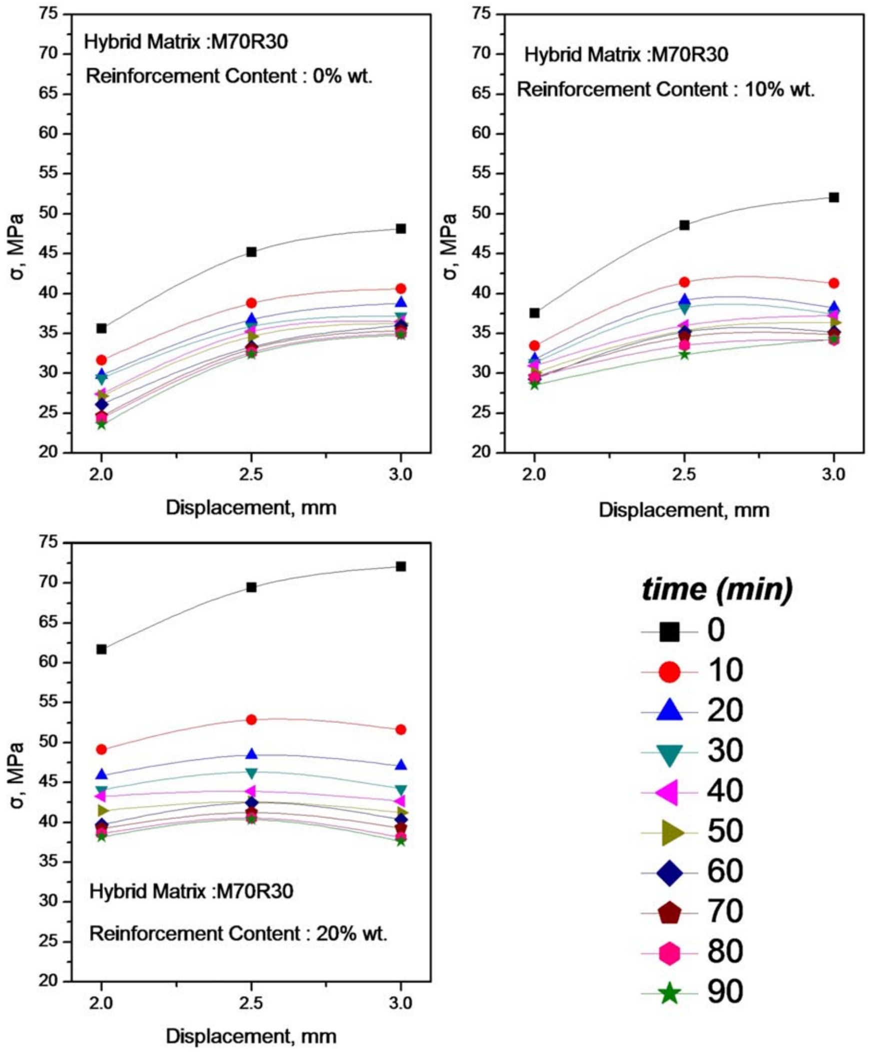

Figure 5. Isochronous curves obtained for the M70R30 hybrid matrix specimens reinforced with short steel fibers at different by weight concentrations. [Color figure can be viewed in the online issue, which is available at wileyonlinelibrary.com.]

Modeling by Means of the Four-Parameter (Burgers) Model

The four parameters Burgers' model[18] is a viscoelastic model consisting of a Maxwell and a Voight model connected in series. A schematic representation of the Burgers model is shown in Figure 6.

Burgers' model can simulate the viscoelastic behavior, which manifests firstly by an instantaneous elastic response followed by viscous behavior and a retarded elastic response.

The overall strain of the model consists of the sum of the individual strains, ε_1 (strain of the Maxwell spring), ε_2 (strain of the Maxwell dashpot), and ε_3 (common strain of the Voight spring and the Voight dashpot):

$$\varepsilon=\varepsilon_1+\varepsilon_2+\varepsilon_3 \tag{1}$$

for which the following expressions are valid:

$$\varepsilon_1=\frac{\sigma}{E_1} \tag{2}$$

$$\frac{d\varepsilon_2}{dt}=\frac{\sigma}{\eta_1} \tag{3}$$

$$\frac{\sigma}{\eta_2}=\frac{E_2}{\eta_2}\varepsilon_3+\frac{d\varepsilon_3}{dt} \tag{4}$$

From the above equations, the following constitutive equation is obtained:

$$\sigma+\left(\frac{\eta_1}{E_1}+\frac{\eta_1}{E_2}+\frac{\eta_2}{E_2}\right)\frac{\mathrm{d}\sigma}{\mathrm{dt}}+\frac{\eta_1\eta_2}{E_1E_2}\frac{\mathrm{d}^2\sigma}{dt^2}=\eta_1\frac{\mathrm{d}\varepsilon}{\mathrm{dt}}+\frac{\eta_1\eta_2}{E_2}\frac{\mathrm{d}^2\varepsilon}{dt^2} \tag{5}$$

Equation 5 can be applied in stress relaxation tests, imposing a known initial deformation, ε_0. Applying the Heaviside step function: $\varepsilon(t)=\varepsilon_0 H(t)$ and the Dirac delta function: $\frac{d\varepsilon(t)}{dt}=\varepsilon_0\ \delta(t)$

$$\frac{d^2\varepsilon(t)}{dt^2}=\varepsilon_0\ \frac{\mathrm{d}\delta(\mathrm{t})}{\mathrm{dt}}$$

Equation 5 can be represented in the following form:

$$\sigma+p_1\frac{d\sigma}{dt}+p_2\frac{d^2\sigma}{dt^2}=q_1\varepsilon_0\delta(t)+q_2\varepsilon_0\frac{d\delta(t)}{dt} \tag{6}$$

where

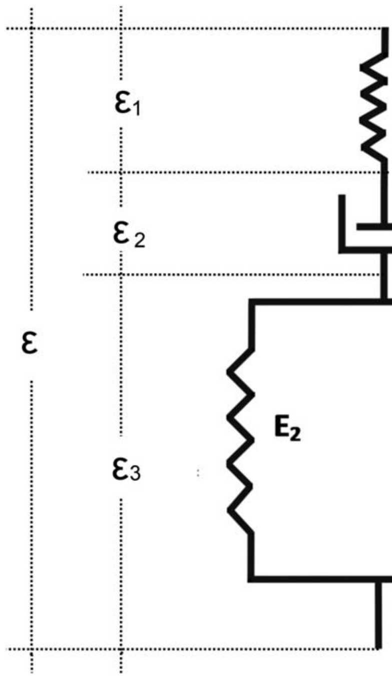

Figure 6. Four parameters (Burgers) model.

$$p_1=\frac{\eta_1}{E_1}+\frac{\eta_1}{E_2}+\frac{\eta_2}{E_2}\quad p_2=\frac{\eta_1\eta_2}{E_1E_2}\quad q_1=\eta_1 \text{ and } q_2=\frac{\eta_1\eta_2}{E_2}$$

Taking the Laplace transforms of eq. (6), we get to eq. (7).

$$\hat{\sigma}+p_1s\hat{\sigma}+p_2s^2\hat{\sigma}=q_1\varepsilon_0+q_2s\varepsilon_0 \tag{7}$$

Solving eq. (7) for $\hat{\sigma}$, we obtain

$$\hat{\sigma}=\frac{\varepsilon_0\,(q_1+q_2s)}{1+p_1s+p_2s^2} \tag{8}$$

Expanding eq. (8) by partial fractions and applying the inverse Laplace transform, the equation of stress relaxation of the Burgers model, can be written as follows:

$$\sigma(t)=\frac{\varepsilon_0}{A}\left[(q_1-q_2r_1)e^{-r_1t}-(q_1-q_2r_2)e^{-r_2t}\right] \tag{9}$$

where $r_1=\frac{p_1-A}{2p_2}$, $r_2=\frac{p_1+A}{2p_2}$, and $A=\sqrt{p_1^2-4p_2}$.

The knowledge of the parameters of eq. (9) allows the calculation of the viscoelastic properties according to the model of Burgers, in the test of stress relaxation, using the set of eq. (10).

$$E_1=\frac{q_2}{p_2},\qquad E_2=\frac{E_1\eta_1^2}{p_1\eta_1E_1-\eta_1^2-q_2E_1},\qquad \eta_2=\frac{q_2E_2}{\eta_1}\quad\text{and}\quad \eta_1=q_1 \tag{10}$$

Figure 7 represents both experimental results and model predictions for the M70R30 hybrid matrix reinforced with 20% wt steel fibers at 2.5 mm displacement. The parameters, E_1, E_2, η_1, and η_2 were obtained by nonlinear fitting of the experimental data and a discussion concerning their values will be given in the sequence of the this article. Thus, it can be concluded that Burger's model can suitably describe the hybrid composites stress relaxation behavior.

In Table IV, four parameters (E_1, E_2, η_1, and η_2) of the Burgers' model are presented as a function of the reinforcement weight

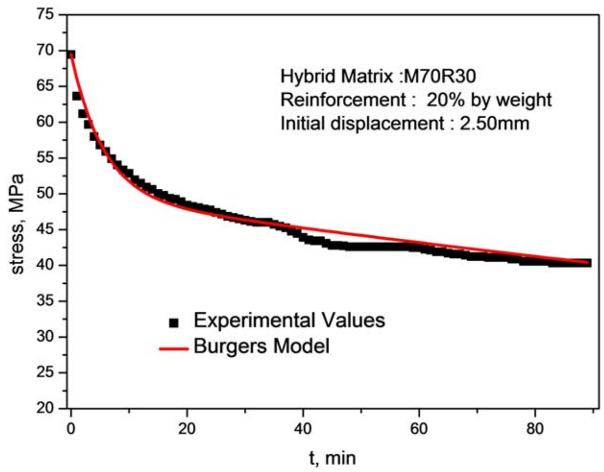

Figure 7. Experimental and calculated, by means of four parameters Burgers model, relaxation stress values for the M70R30 hybrid matrix reinforced with 20% wt steel fibers at 2.5 mm displacement. [Color figure can be viewed in the online issue, which is available at wileyonlinelibrary.com.]

fraction and for three different initial deformations applied to the specimens.

The model parameters E_1, E_2, η_1, and η_2 obtained by nonlinear fitting of the experimental data are shown in the above-mentioned bar diagrams. The first instantaneous stress arises from the spring or the elastic element (E_1) and later time dependent stress comes from the parallel spring and dashpot (η_2) and from the viscous dashpot flow (η_1). According to this model, the modulus (E_1) of the Maxwell spring increases with the increase in filler weight fraction and this is attributed to the stiffening of the material as the hybrid matrix is further reinforced. The retardant elasticity (E_2) however showed a decrease with the increase in filler content. On the other hand, viscosity, η_1, decreased with the increase in the reinforcement concentration, with the only exception the case of R60M40 hybrid matrix (the last case) subjected to the maximum deformation of 3.0 mm. In this specific case, an increase in the viscosity η_1 with filler weight fraction was observed. Finally, parameter η_2 remained almost constant in all cases. These variations can be correlated with respective microstructural changes of the composites investigated, which, in turn, are depended on the value of the initial deformation applied to the specimen.

Modeling by Means of the R.P.M. Model

RPM model, developed by G. C. Papanicolaou, has been used for the predicting the residual values of the mechanical properties of materials previously subjected to different types of damages such as those resulted from the application of open gas flame exposure,[19] notch induction,[20] and the application of thermal fatigue.[21]

Because constant deformation imposed results in a decrease in stress, a modified form of the RPM model can be used to describe this decrease. The relationship proposed is of the form:

$$\frac{\sigma_t}{\sigma_0}=s+(1-s)e^{-s\lambda} \tag{11}$$

Table IV. Variation of Burger's Model Parameters with Reinforcement Content and Initial Displacement

Hybrid matrix	Reinforcement by weight content, %	Initial displacement (mm)	E_1	η_1	E_2	η_2
M60R40	0.00	2.00	4.87 E +03	7.00 E +06	3.50 E +04	4.50 E +05
M60R40	10.00	2.00	5.36 E +03	1.50 E +06	3.00 E +04	1.40 E +05
M60R40	20.00	2.00	5.67 E +03	1.10 E +06	2.50 E +04	1.60 E +05
M60R40	0.00	2.50	4.84 E +03	1.00 E +07	4.00 E +04	4.50 E +05
M60R40	10.00	2.50	5.59 E +03	9.50 E +05	3.00 E +04	1.60 E +05
M60R40	20.00	2.50	6.26 E +03	3.60 E +06	2.70 E +04	2.30 E +05
M60R40	0.00	3.00	4.69 E +03	1.20 E +06	4.00 E +04	1.60 E +05
M60R40	10.00	3.00	5.66 E +03	4.00 E +06	1.40 E +04	1.90 E +05
M60R40	20.00	3.00	6.13 E +03	6.00 E +06	1.20 E +04	1.90 E +05
M70R30	0.00	2.00	5.53 E +03	3.25 E +06	4.40 E +04	4.50 E +05
M70R30	10.00	2.00	5.98 E +03	4.00 E +06	3.50 E +04	3.00 E +05
M70R30	20.00	2.00	9.16 E +03	2.45 E +06	3.40 E +04	1.80 E +05
M70R30	0.00	2.50	5.76 E +03	3.50 E +06	2.50 E +04	2.20 E +05
M70R30	10.00	2.50	6.25 E +03	4.00 E +06	2.35 E +04	2.50 E +05
M70R30	20.00	2.50	8.19 E +03	2.50 E +06	1.60 E +04	1.90 E +05
M70R30	0.00	3.00	5.40 E +03	2.00 E +06	3.50 E +04	2.00 E +05
M70R30	10.00	3.00	5.56 E +03	2.80 E +06	1.80 E +04	1.20 E +05
M70R30	20.00	3.00	7.02 E +03	1.50 E +06	1.60 E +04	1.00 E +05

with

$$s=\frac{\sigma_\infty}{\sigma_0} \tag{12}$$

and

$$\lambda=\frac{t}{\tau} \tag{13}$$

where $\sigma_t=$ stress value at time t, $\sigma_0=$ initial stress value (at zero time), $\sigma_\infty=$ the long-term stress value, $\tau=$ relaxation time, and $t=$ current time.

According to eqs. (11–13), relationship eq. (11) can be written as

$$\frac{\sigma_t}{\sigma_0}=s+(1-s)e^{-s(t/\tau)} \tag{14}$$

As it can be seen from relation eq. (14), two experimental points are only needed for the prediction of the whole stress relaxation curve. These two points should be selected in the following way. The first out of them should be a point corresponding to short times, that is, at the very beginning of the relaxation test where the material behavior is almost purely elastic, whereas the second point should be a point close to the end of relaxation test where the materials' behavior is purely viscoelastic and where the system is in a state of equilibrium.

Results obtained by means of the RPM model for the case of M60R40 hybrid matrix reinforced with 10 wt % steel fibers and for displacement 2.50 mm are shown in Figure 8. As can be seen, RPM predicts well the relaxation behavior of all the materials investigated.

The variation of the relaxation time τ as a function of the applied displacement and the filler volume fraction is shown in Figures 9 and 10, respectively. From these figures, a linear decrease of the relaxation time with either applied displacement or filler content is observed.

CONCLUSIONS

In the current work, the flexural stress relaxation behavior of a hybrid matrix–fiber reinforced building material was investigated. Hybrid matrix consisted of epoxy resin mixed with fine

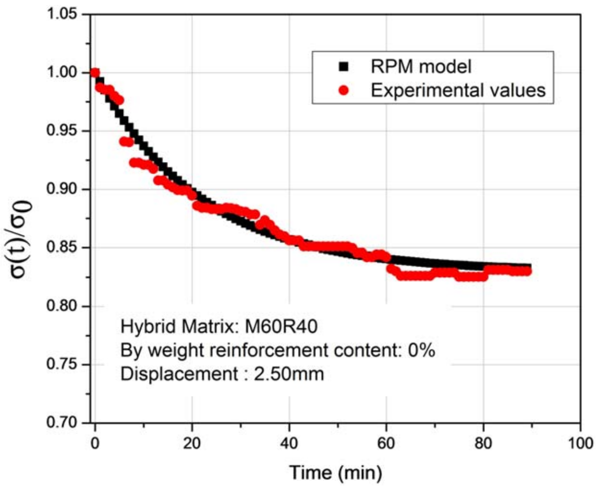

Figure 8. Application results of the RPM model for the case of M60R40 hybrid matrix reinforced with 10 wt % steel fibers and for displacement 2.50 mm. [Color figure can be viewed in the online issue, which is available at wileyonlinelibrary.com.]

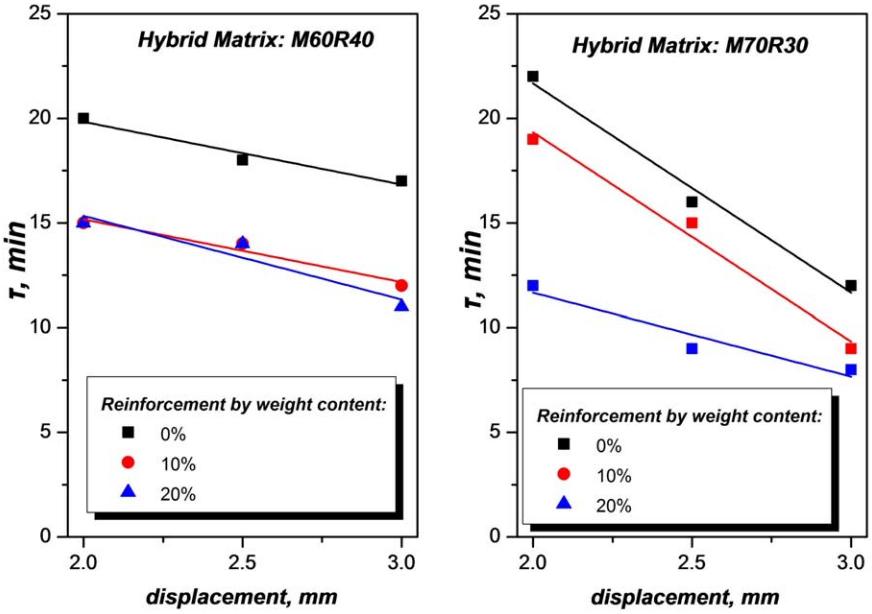

Figure 9. Relaxation time τ, as derived from the application of the RPM model, versus applied displacement for the hybrid matrices M60R40 and M70R30. [Color figure can be viewed in the online issue, which is available at wileyonlinelibrary.com.]

marble sand, whereas short steel fibers at different weight fractions were used as reinforcement.

In all cases, a nonlinear viscoelastic behavior of the materials manufactured and tested, under flexural stress relaxation configuration, was observed. Despite the nonlinear viscoelastic behavior observed, Burger's model can describe adequately well the hybrid composites stress relaxation behavior. The four Burgers' model parameters variation with filler content give a better insight on the viscoelastic behavior of the hybrid composites manufactured and tested. RPM model can predict well the viscoelastic behavior of the aforementioned materials. Model parameters have a physical meaning, whereas their values as calculated for each displacement applied and for the different reinforcement weight fractions give a complementary insight on the materials viscoelastic behavior.

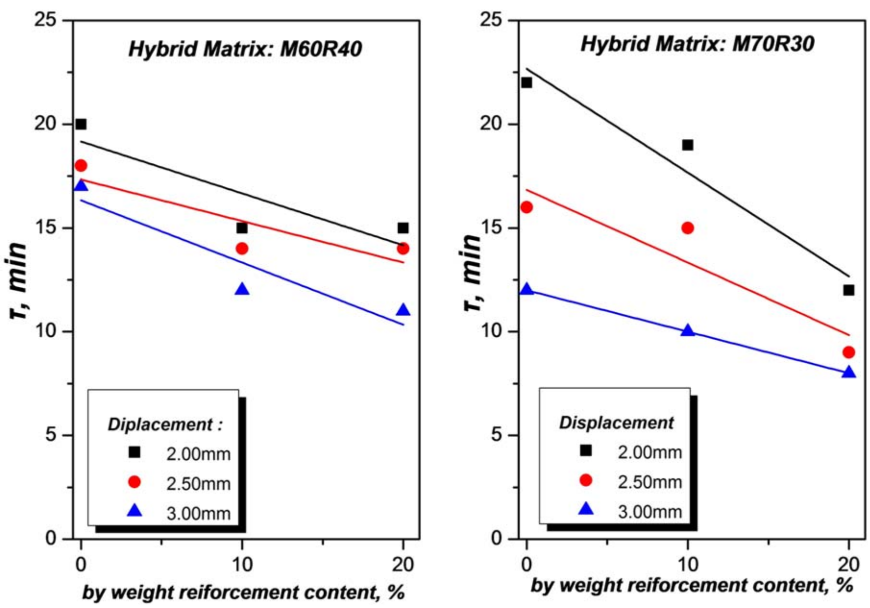

Figure 10. Relaxation time τ, as derived from the application of the RPM model, versus reinforcement weight fraction, for the hybrid matrices M60R40 and M70R30. [Color figure can be viewed in the online issue, which is available at wileyonlinelibrary.com.]

REFERENCES

1. Hollaway, L. C. *Adv. Struct. Eng.* **2010**, *13*, 927.
2. El-Enein, H. A.; Azimi, H.; Sennah, K.; Ghrib, F. *Constr. Build. Mater.* **2014**, *57*, 126.
3. Mohamed, N.; Farghaly, A. S.; Benmokrane, B.; Neale, K. W. *J. Compos. Constr.* **2014**, *18*, 04013044.
4. Li, J.; Bakoss, S. L.; Samali, B.; Ye, L. *Compos. Struct.* **1999**, *47*, 805.
5. Garden, H. N.; Hollaway, L. C. *Compos. B.* **1998**, *29*, 411.
6. Bedard, C. *Concr. Int.* **1992**, *14*, 55.
7. Ahmad, S.; Elahi, A.; Barbhuiya, S.; Farooqi, Y. *Mater. Struct.* **2013**, *46*, 1547.
8. Kulakowski, P. M.; Pereira, M. F.; Dal Molin, C. C. D. *Constr. Build. Mater.* **2009**, *23*, 1189.
9. Yang, K. H.; Seo, E. A.; Tae, S. H. *Environ. Impact Asses.* **2014**, *46*, 43.
10. Ramezanianpour, A. A.; Ghahari, S. A.; Esmaeili, M. *Constr. Build. Mater.* **2014**, *58*, 138.
11. Bhutta, M. A. R.; Maruya, T.; Tsuruta, K. *Constr. Build. Mater.* **2013**, *43*, 50.
12. Assmann, A.; Reinhardt, H. W. *Cem. Concr. Res.* **2014**, *58*, 179.
13. Xu, F.; Zhou, M.; Chen, J.; Ruan, S. *Constr. Build. Mater.* **2014**, *63*, 142.
14. Yeon, K. S.; Yeon, J. H.; Choi, Y. S.; Min, S. H. *Constr. Build. Mater.* **2014**, *63*, 125.
15. Vidales, J. M. M.; Narvaez Hernandez, L. N.; Lopez, J. I. T.; Flores, E. E. M.; Hernandez, L. S. *Constr. Build. Mater.* **2014**, *65*, 376.
16. Fowler, D. W. *Cem. Concr. Comp.* **1999**, *21*, 449.
17. Papanicolaou, G. C.; Lagas, G.; Papadimitropoulos, K.; Ioannou, A. *J. Appl. Polym. Sci.* **2012**, *124*, 1081.
18. Liu, Y.; Dai, Q.; You, Z. *J. Eng. Mech.* **2009**, *135*, 324.
19. Papanicolaou, G. C.; Lagas, G.; Mimigiannis, N. I. *J. Appl. Polym. Sci.* **2012**, *127*, 2724.
20. Papanicolaou, G. C.; Mouzakis, D. E.; Kosmidou, T. H. V.; Economopoulos, G. *Polym. Compos.* **2006**, *27*, 177.
21. Papanicolaou, G. C.; Koutsomitopoulou, A. F.; Sfakianakis, A. *J. Appl. Polym. Sci.* **2012**, *124*, 67.